HEFAT2011
8th International Conference on Heat Transfer, Fluid Mechanics and Thermodynamics
11 – 13 July 2011
Pointe Aux Piments, Mauritius

PARAMETRIC INFLUENCE OF OPEN-CELL METAL FOAM ON THERMAL AND HYDRAULIC PERFORMANCE

De Jaeger P.*, T'Joen C., Huisseune H., Ameel B. and De Paepe M.
*Author for correspondence
Department of Flow, Heat and Combustion Mechanics,
Ghent University - Ugent,
Gent,
Belgium,
E-mail: peter.dejaeger@ugent.be

ABSTRACT

Heat transfer in open-cell metal foams has been studied extensively, based on porous media physical properties. In this contribution, these physical properties are described as a function of the fundamental foam parameters, starting from the foam cell structure.

The governing equations dealing with the multi-scale issues are introduced to rigorously derive the associated porous parameters. Experimental characterisation allowed to relate these parameters to the structural characteristics. This allows to perform a parametric study with respect to thermal and hydraulic performance for a fixed flow arrangement and application, revealing an optimum.

INTRODUCTION

Air side thermal resistance is in many applications overwhelming, possibly contributing 90% of the total thermal resistance. Techniques to decrease the air side thermal resistance are commonly based on augmenting heat transferring surface area and minimizing the formation of boundary layers. This has lead to the development of a variety of fin types. In many applications, louvered fins can be considered industry standard. Further improvement of the fins is under investigations with for example the addition of vortex generators. Another approach is looking at totally new structures, such as open-cell metal foams.

These materials consist of a finite number of interconnected polyhedral cells through pores in their faces. This results in a single fluid domain, spanning the complete foam volume. Solid struts form the borders around the pores and connect the vertices of the solid matrix. Also the solid matrix is a continuous volume throughout the foam volume, as depicted in Figure 1. Such materials are known to have interesting structural and functional properties, such as:

- High porosity (> 0.85 when uncompressed)
- High interfacial surface area between the solid and fluid phase, per unit volume. This is also called surface-to-volume ratio. Typical values range from 400 to over 2500 m^{-1} when uncompressed.
- Relatively high strength and toughness, giving them structural stability and good impact energy absorption
- Good noise attenuation
- Excellent fluid mixing due to tortuous flow paths
- High gas permeability

NOMENCLATURE

a_1, a_2	[-]	Strut cross-sectional and axial shape factors
A_0	[m²]	Strut cross-sectional surface area at the middle
c_p	[J/kgK]	Specific heat
h	[W/m²K]	Interfacial heat transfer coefficient
H	[m]	Height of foam volume
k	[W/mK]	Thermal conductivity
l	[m]	Strut length
L	[m]	Flow depth through the foam
Nu	[-]	Nusselt number
Pr	[-]	Prandtl number
Re	[-]	Reynolds number
T	[°C]	Temperature
v	[m/s]	Superficial velocity
W	[m]	Width of foam volume
x, y, z	[m]	Cartesian axis direction

Special characters

α	[-]	Volume fraction ratio
$\mathcal{A}$	[m]	Half centre-to-centre offset distance between neighbouring cooling inserts in the x direction
$\mathcal{B}$	[m]	Half centre-to-centre offset distance between neighbouring cooling inserts in the y direction
$\mathcal{b}$	[m]	Half y directional dimension of rectangular cooling insert
ε	[-]	Relative $E_{\%}$ value in terms of maximum $E_{\%}$
γ	[-]	Ratio between thermal conductivities of cooling insert and the heat-generating medium
$\mathcal{Z}$	[m]	Half z directional dimension of rectangular cooling insert

Subscripts

C	Cooling layer
eff	Volumetric effective expression
ext	External: Towards external heat sink
int	Internal: Between cooling and heat-generating layers
M	Heat generating medium
max	Maximum
0	Ambient or reference

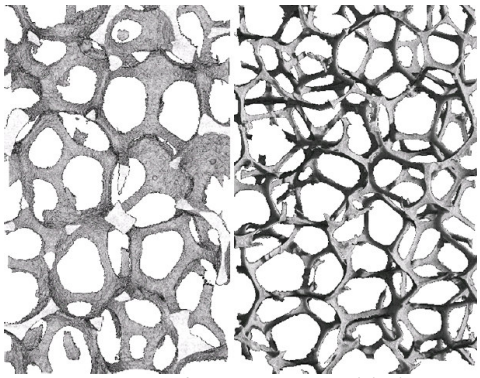

Figure 1 Two foam structure with the same cell size but manufactured with different strut thickness

The relatively small size of the struts prevents for large boundary layers to form. Furthermore, the splitting and rejoining of flow streamlines when passing a strut introduce additional hydrodynamic mixing. When using highly thermal conductivity materials (such as aluminum or copper), combined with the inherently high interfacial surface area, makes foam potential candidates for compact heat exchangers. However, the hydrodynamic mixing has its consequences on pressure drop. A trade-off has to be made on the foam's geometrical parameters to maximize heat transfer for a given pressure drop. This trade-off is discussed in this paper for one flow arrangement and heat exchanger setup.

FOAM STRUCTURAL REPRESENTATION

Foam structure has been described in a variety of models, ranging from a cubic unit cell representation to a fully three-dimensional virtual reconstruction via micro-computed tomography scanning (µCT scan). When aiming on a macroscopic analysis, i.e. on length scale above cell dimension, it is found that foams bare a high degree of regularity although they are inherently stochastic. This is expressed in the coefficient of variation of the cell dimension, measuring less than 5%. This justifies a periodic unit cell representation; at least when a macroscopic analysis is intended. More advanced models are required when the microscopic heterogeneity needs to be studied, such as Laguerre tessellations [1] or the µCT scan reconstruction.

The structural model is based on a Kelvin cell representation, with struts placed on the resulting wire-frame representation. The orthotropic cell structure is characterised by two cell diameters, corresponding to the averaged diameters of an ellipse encompassing a cell. The struts are modelled by generalising the characterisation of Jang et al. [2], as depicted in Figure 2. They published a quartic variation of strut cross-sectional surface area with respect to non-dimensionalised axial position.

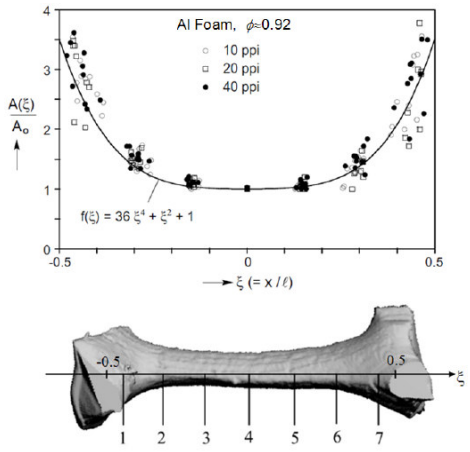

Figure 2 Strut shapes are modelled by generalizing the characterisation of Jang et al. [2]

Generalising is achieved by proposing following quartic relation:

$$f(\xi) = a_2\xi^4 + \xi^2 + 1, \quad \text{with } \xi = \frac{x}{l} \text{ and } -\frac{l}{2} < x < \frac{l}{2}, \quad (1)$$

with $A(\xi)$ is the cross-sectional surface area at dimensionless position ξ, x is the axial coordinate and l the strut length between the two nodes it connects. Based on µCT scan data, the axial shape factor a_2 is related to porosity ϕ:

$$a_2 = 17342\phi^2 - 31809\phi + 14622 \quad (2)$$

Remark that the manufacturing process is based on a thickening a polyurethane preform with a wax layer [3]. This thickened structure is subsequently replicated via an investment casting technique in the gestured metal. This is important to know, as the thickening does not obey surface minimization principles or other conventional physical laws. Consequently, generated foam models will always bare a form of empiricism.

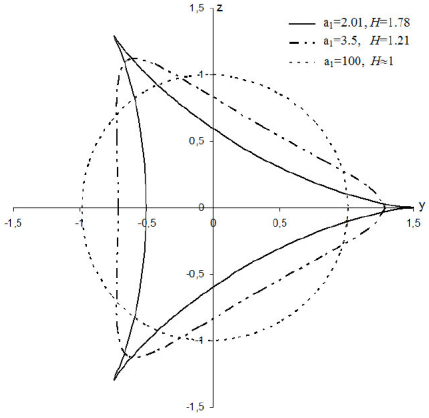

Figure 3 Strut cross-sectional shape for various shape factors a_1

The strut cross-sectional shape is parameterised via following formulas:

$$y(x,\varphi) = R(x)\left(\cos(\varphi) + \frac{\cos(2\varphi)}{a_1}\right)$$
$$z(x,\varphi) = R(x)\left(-\sin(\varphi) + \frac{\sin(2\varphi)}{a_1}\right) \qquad (3)$$

where $R(x)$ is a measure of the strut cross-sectional size, resulting in the earlier introduced axial strut shape variation. The struts are represented in a cylindrical coordinate system with angle φ. The strut cross-sectional shape factor a_1 is also empirically correlated with porosity via the Heywood factor (HW) [4], defined as the ratio of the strut cross-section perimeter to the equivalent perimeter of a circle with the same surface area. The Heywood factor correlation reads:

$$HW = 0.971(1-\phi)^{-0.09} \qquad (4)$$

Figure 3 depicts the cross-sectional shapes for three factors a_1 with accompanying Heywood factor.

Following an iterative scheme, both shape factors a_1 and a_2 can be adjusted to the resulting porosity of a generated foam structure, based on the three input parameters (two cell diameters and strut cross-sectional surface area). Indeed, by performing a volumetric integration of the solid phase, porosity is fully determined by the introduced structural parameters. The resulting final porosity and interfacial surface-to-volume ratio σ_0 is compared to experimental data obtained via µCT scan. The latter is depicted in Figure 4, yielding a good agreement.

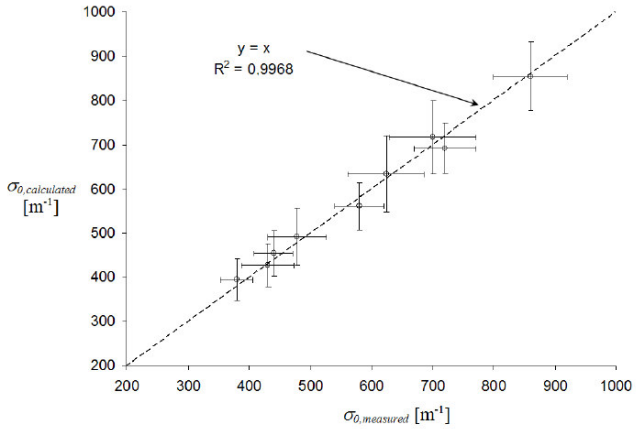

Figure 4 Experimental validation of the geometrical foam model, representing a good agreement for the interfacial surface-to-volume ratio σ_0.

FROM MICROSCOPIC TO MACROSCOPIC

Microscopic thermal and hydrodynamic phenomena have typical length scales below the cell dimensions. Solving these by directly applying Navier-Stokes equations and energy conservation can only be done on a limited representation of the foam structure, well below the number of cells in an application. To tackle this multi-scale problem, the conventional equations are integrated over a representative elementary volume (REV) of the solid matrix. The details of this procedure can be found in [5]. The resulting equations however inherently have terms which transport microscopic behavior to the macroscopic scales of interest. However, as the microscopic phenomena are unknown, these need to be modeled, which forms the closure problem. Assuming fully developed flow and steady flow on macroscopic scale, the momentum equation in one dimension reads:

$$\phi \nabla P = \mu_e \nabla^2 v + \mu \kappa^{-1} v + \rho \beta v^2, \qquad (5)$$

where P [Pa] is pressure, μ_e [Pa.s] is effective viscosity, v [m/s] superficial velocity, μ [Pa.s] molecular viscosity, κ [m^2] permeability, ρ [kg/m^3] fluid density and β [-] inertial loss factor. The effective viscosity of the first term in equation (5), i.e. the Brinkman term, takes momentum dispersion in account from the splitting and rejoining of flow streamlines when they are forced to pass a strut. Remark that this is a different mechanism than the Reynolds stress which occurs in turbulent flow and is modeled via the eddy viscosity. To make the distinction clear, the intended dispersion is also referred to as mechanical dispersion. Permeability is introduced via the second term in equation (5), also called Darcy term, and stems from the closure term which takes viscous friction on the solid-fluid interfacial surface area in account. The last term in equation (5), or Forchheimer correction term, introduced the inertial factor which accounts for the form drag (or pressure drag) induced by a flow passing the struts.

The energy equations for fluid and solid phase read after averaging:

$$(\rho c_p)\mathbf{v}.\nabla T = \nabla k_e^f.\nabla T^f - \sigma_0 h(T^f - T^s)$$
$$0 = \nabla k_e^s.\nabla T^s + \sigma_0 h(T^f - T^s), \qquad (6)$$

with the superscripts f and s respectively denoting fluid and solid phase, T [°C] is the averaged temperature in the REV, k_e [W/mK] is effective thermal conductivity and h [W/m^2K] is the interfacial heat transfer coefficient. The transport of microscopic thermal phenomena to the macroscopic scale is ensured by the effective thermal conductivities and interfacial heat transfer coefficient. Solid phase effective thermal conductivity has to take the structural tortuosity in account, as the thermal path through the struts is considerably longer than a straight connection between two nodes. Concerning the fluid phase, effective thermal conductivity depends on the fluids molecular properties, but also on hydrodynamic mixing. The latter is termed thermal dispersion and is based on the same physical phenomena like the earlier discussed momentum dispersion.

MACROSCOPIC PROPERTIES

The introduced macroscopic properties (or porous properties) transport the microscopic phenomena to the scale of interest. They depend on the foam's structure and flow conditions. The former have been clearly defined. Concerning the flow conditions, a rectangular channel flow arrangement is considered. The foam sample dimensions are H=4.85mm height, L=40 mm flow depth and W=100mm width (see Figure 6). To find an expression for the permeability and inertial loss

factor, pressure drop is experimentally determined for foam with their geometrical characterization given in Table 1.

Nr	d_1 [mm]	d_2 [mm]	A_0 [10^{-1}mm^2]	ϕ [-]	σ_0 [m^{-1}]
1	4.22	6.23	0.998	0.932	440
2	2.52	3.78	0.463	0.913	860
3	2.77	4.15	0.377	0.937	720

Table 1 Foam samples used in this paper

Following Auriault [6], the Brinkman term in equation (5) can not be neglected. However, when performing the pressure drop measurement in the described flow arrangement, the effects of effective viscosity will inherently be present in the Darcy and Forchheimer terms. As such, the obtained correlations are only valid for the discussed flow arrangement.

The pressure drop is correlate via an empirically tuned Ergun-type correlation, given by [7]:

$$\frac{\Delta P}{L} = \alpha_c \left[\frac{(1-\phi)^2}{\phi^3 D} \right]^{m_c} \mu v + \rho \beta_c \left[\frac{(1-\phi)^2}{\phi^3 D} \right]^{n_c} v^2, \qquad (7)$$

with D a structural parameter, calculated as the ratio of the equivalent diameter yielding the same cross-sectional surface area as A_0 and the smallest cell diameter. This implicitly means that the flow is normal to directions of the foam's largest diameter. The coefficients with subscript c are determined by minimizing the residual of equation (7) with experimental data obtained via the first sample. The model is validated by comparing calculated pressure drop per unit flow depth with measured data of foam samples 2 and 3. The result is given in Figure 5, showing appreciable agreement.

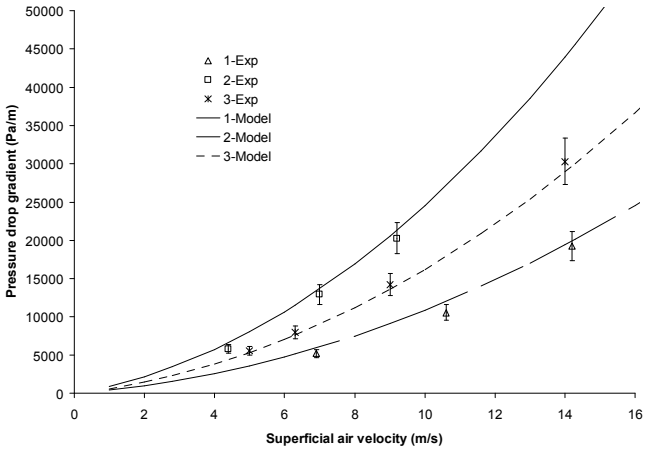

Figure 5 Experimental validation of pressure drop correlation

By comparing the proposed pressure drop correlation (7) with momentum equation (5) and assuming that the Brinkman effects are included in the pressure drop correlation, it is possible to derive an empirical formula for both permeability and inertial coefficient. Furthermore, as porosity is related to the introduced structural parameters, both porous properties are directly linked to them. This allows to evaluate pressure drop with respect to the foam structure.

To derive a formulation of thermal properties with respect to the foam's structural parameters, a measure for the effective thermal conductivities of both phases and the interfacial heat transfer coefficient is required. For the latter, Calmidi and Mahajan [8] proposed the Zukauskas correlation for cylinders in cross-flow configuration. This is also employed in this paper. An equivalent diameter, yielding the same strut cross-sectional surface area as A_0 is used as characteristic length because the flow is treated as external flow. The resulting correlation is given by:

$$Nu = 0.52 \left(\frac{\rho d_e v}{\mu \phi} \right)^{0.5} \mathrm{Pr}^{0.37}, \qquad (8)$$

with Pr the Prandtl number of air. Notice the porosity occurs in the Reynolds number as the velocity near the strut is considered. This correlation is valid for Re between 40 and 1000.

For the effective thermal conductivity of the solid phase, the empirical correlation of Bhattacharya et al. [9] is used. Comparing the thermal conductivity of the solid phase (k_s=220 W/mK for Aluminum 1050 alloy) with air ($k_f \approx 0.03$W/mK), it is clear that the solid phase overwhelms, even when it is weighted with their respective volumetric content. The resulting correlation is simply given by:

$$k_e^{\,s} = 0.35\,(1-\phi)\,k_s \qquad (9)$$

Recalling that porosity is a known function of the three structural foam parameters, also effective solid thermal conductivity is fully parameterized.

The last parameter to deal with is fluid effective thermal conductivity. Two contributions are captured with this: molecular thermal conductivity of air and dispersion. For the former, the NIST database provides the necessary data to relate it with temperature. The latter however depends on the foam structure. Calmidi and Mahajan [8] have used following correlation:

$$\frac{k_d}{k_e^s} = 0.06 Pe_\kappa, \qquad (10)$$

with the Peclet number based on the square root of the foam's permeability. Because permeability was earlier related to the foam's structural parameters, all porous properties are now fully parameterized.

THERMO-HYDRAULIC PARAMETER STUDY

Solving the momentum and energy equation now allows to evaluate thermal and hydraulic performance with respect to the structural parameters. A one-dimensional solution is obtained by assuming that conductive heat transfer in the solid phase only occurs in the normal direction with respect to the walls confining the solid matrix. Air flow is also considered one-dimensional, but parallel to the solid walls. This assumption is

only valid because the foam height is 4.85mm with isothermal plates on top and bottom of the foam.

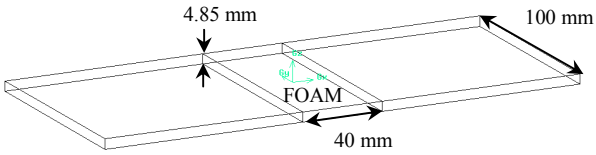

Figure 6 Flow arrangement and foam volume

Assuming developed flow through the foam (neglecting entrance and exit effects), Kaviany [10] proposed an analytical solution of equation of the equation (5). As such, the velocity boundary layer near the no-slip top and bottom walls is correctly accounted for. This velocity profile is used in the thermal property equations (8 and 10).

A constant temperature of 80°C is applied as boundary condition on both the top and bottom wall of the foam volume. The temperature of the air entering the system is set at 20°C.

Under the assumption of a constant pressure drop across the foam, it is now possible compute the heat transfer in the introduced configuration. Altering the structural parameters of the foam adapts both flow properties, i.e. permeability and inertial loss factor. Consequently, for the given pressure drop, the velocity profile will be adjusted. As thermal properties depend on this velocity, also the interfacial heat transfer coefficient and thermal dispersion are altered. Thus thermal performance takes the hydraulic characteristics of the foam in account. Doing so, it is possible to present a single graph where both thermal and hydraulic performance are captured by the heat transfer, expressed in W. This is presented in Figure 7.

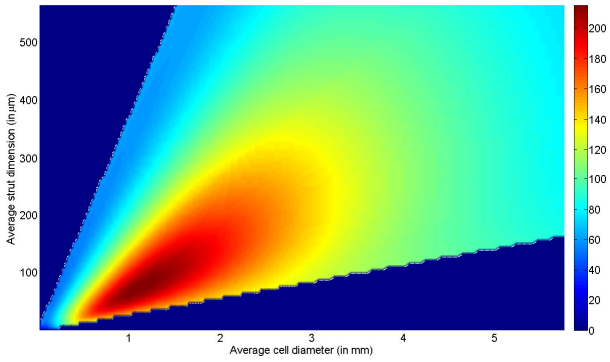

Figure 7 Influence of foam structural parameters on heat transfer in W, under the condition of constant pressure drop (300 Pa).

The graph is truncated for foams with porosity below 0.75 or above 0.98 because these are considered non-physical; at least in uncompressed condition. The proposed procedure suggests an optimal foam structure with averaged cell diameter of 1.2mm and average equivalent strut diameter of 70µm for the discussed flow arrangement. An experimental validation of this foam structure is not possible because the available manufacturing technique (investment casting) does not allows to construct this type of foam. However, the differences between the three foams presented in Table 1 are sufficient to compare the modeling results with experimental data.

For the latter, three compact heat exchangers are manufactured with the channels between the flat tubes having double width of the discussed arrangement thus far. The foam is bonded on flat tubes with a single epoxy (Bondmaster ESP 108). Although this introduces a considerable thermal resistance, it offers great flexibility for manufacturing prototypes which is the reason why it was used in this study. The resulting heat exchanger with the third foam presented in Table 1 is depicted in Figure 7. The larger width and the numerous tubes allows to minimize boundary effects.

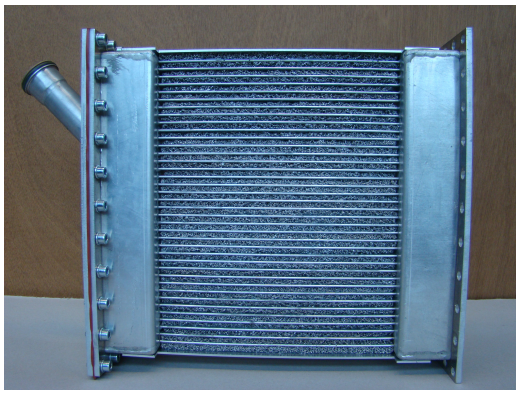

Figure 8 Compact heat exchanger with open-cell aluminium foam, used to validate the parametric study

A typical windtunnel campaign is ran to characterize both thermal and hydraulic performance. Heat balance between water and air was closed within 5% under all circumstances. Data processing is done via the log-mean temperature difference method, with the appropriate F-factor chosen from Shah et al. This results in an overall thermal resistance of the compact heat exchangers. After subtracting the internal convection resistance on water side and tube wall resistance, an external thermal resistance of the system is obtained. However, the bonding method with a single epoxy adds a considerable thermal resistance as the thermal conductivity of this substance is 0.67 W/mK. A conservative estimation of the epoxy layer thickness allows to evaluate this additional thermal resistance, as is also applied in T'Joen et al. [11]. Subtracting this from the total external resistance leaves the air side contribution of the foam.

Applying the same operating conditions of the earlier discussed theoretical treatment allows to compute the hypothetical heat transfer which can be obtained with the experimentally tested compact heat exchangers. The result is depicted in Figure 9, indicating that the predicted values are within measurement accuracy. For the latter, a detailed uncertainty analysis is performed, following the recommendations of Moffat et al. The found uncertainty is 15%, mainly due to the bonding layer. A clear correlation between measured and computed heat transfer is retrieved.

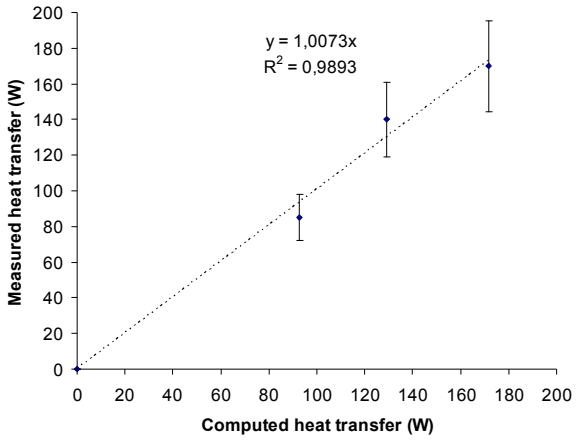

Figure 9 Validation for the three foams presented in Table 1, showing a clear correlation between both data sets.

The results show that under the condition of limited foam height, a clear optimum can be found. This can also be seen in Figure 7, where too thin struts make the heat transfer decrease, although pressure drop also decreases. The conductive resistance of the solid matrix overwhelms (fin efficiency drops). On the other hand, when struts are too thick, there is a pressure drop penalty. The found optimum clearly demonstrates there is a fragile trade-off to make.

CONCLUSION

A parametric study of open-cell aluminium foam compact heat exchangers is presented. In first instance, a structural model is derived which introduces the necessary foam parameters. Subsequently, averaging the conventional conservation laws is discussed as this resolves the multi-scale issue when dealing with complex structures. Note that this approach also could be applied on fins as these can be considered an anisotropic porous medium.

The up-scaling introduces porous properties which transport microscopic phenomena to the macroscopic scales. Available models from literature are applied and altered in order to relate the porous properties with the foam's structural parameters. Doing so, a thermal and hydraulic analysis allows to indirectly asses the influence of the structural parameters. After experimentally validating this influence for three cases, it is clear that a fragile optimal foam structure can be derived for the given flow arrangement.

Further investigation is required to generalize this approach for other flow arrangements.

ACKNOWLEDGEMENT

The authors express their gratitude to Bekaert for the close cooperation. The Institute for the Promotion of Innovation by Science and Technology (IWT Vlaanderen) is greatly acknowledged for their financial support (IWT-090273).

REFERENCES

[1] Redenbach C., Modelling foam structure using random tessellations, *Proceedings of the 10th European Conference of International Society for Stereology,* 2009

[2] Jang, W., Kraynik, S., Kyriakides, On the microstructure of open-cell foams and its effect on elastic properties, *International Journal of Solids and Structures* Vol. 45, 2008, pp. 1845-1875

[3] Walz, D. D., Cordova, R., Method of making an inorganic reticulated foam structure, *Energy Research Generation Inc.,* Oakland, Ca, USA, 1967

[4] Schmierer, E. N., Razani, A., Self-consistent open-celled metal foam model for thermal applications, *Journal of Heat Transfer,* Transactions of the ASME, 128, No. 11, 2006, pp. 1194-1203

[5] Whitaker, S., The method of volume averaging, *Kluwer Academic Publishers,* Dordrecht, The Netherland, 1998

[6] Auriault, J. L., On the domain of validity of Brinkman's equation, *Transport in Porous Media*, Vol. 79, No. 2, 2008, pp. 215-223

[7] Hernandez, A. R. A., Combined flow and heat transfer characterization of open cell aluminum foams, *Master's thesis,* University of Puerto Rico Mayaguez Campus, 2005

[8] Calmidi, V. V., Mahajan, R. L., Forced convection in high porosity metal foams, *Journal of Heat Transfer,* Transactions of ASME, Vol. 122, No. 3, 2000, pp. 557-565

[9] Bhattacharya, A., Calmidi, V. V., Mahajan, R. L., Thermophysical properties of high porosity metal foams, *International Journal of Heat and Mass Transfer,* Vol. 45, No. 5, 2002, pp. 1017-1031

[10] Kaviany, M., Principles of Heat Transfer in Porous Media, *Mechanical Engineering Series,* Springer-Verlag New York, Inc., Second edition, 1995.

[11] T'Joen, C., De Jaeger, P., Huisseune, H., Van Herzeele, S., Vorst, N., De Paepe, M., Thermo-hydraulic study of a single row heat exchanger consisting of metal foam covered round tubes, *International Journal of Heat and Mass Transfer,* Vol. 53, No. 15, 2010, pp. 3262-3274